University of Tehran Press

Pollution

Print ISSN: 2383-451X
Online ISSN: 2383-4501

https://jpoll.ut.ac.ir/

Distribution of Natural Radionuclides and their Radiological Risks on Agricultural Soil Samples collected from Yemen

Maher Taher Hussien [1] | Ghada Salaheldin [2] ✉* | Haby Salaheldin Mohamed [3] | Howaida Mansour [4]

1. Physics Department, Faculty of Education Yafea, Aden University, Aden, Yemen.
2. Physics Department, Faculty of Science, Assiut University, Assiut 71516, Egypt.
3. Geology Department, Faculty of Science, Assiut University, Assiut 71516, Egypt.
4. Physics Department, Faculty of Women for Arts, Science and Education, Ain Shams University, Egypt.

Article Info

Article type:
Research Article

Article history:
Received: 10.06.2022
Revised: 3.10.2022
Accepted: 01.11.2022

Keywords:
Natural radionuclides
Radiological parameters
Gamma spectroscopy

ABSTRACT

The main objective of the current study is to determine the distributions of the specific radioactivity concentrations (^{226}Ra, ^{232}Th and ^{40}K) from terrestrial sources using gamma spectroscopy system (HPGe-detector). Forty (40) agricultural soil samples were collected from Wadi Al-Hussini and Tuban in Yemen. The study locations are famous for exporting coffee all over the world. The average of radio-concentrations of ^{226}Ra, ^{232}Th and ^{40}K were 61.95±11.57, 32.33±8.03 and 1045.17±153.47 Bq/kg for Wadi Al-Hussini and 65.20±11.59, 50.95±9.80 and 1078.13±157.57 Bq/kg for Tuban, respectively. The obtained results are higher than the average worldwide values reported by UNSCEAR. So, it is not acceptable with global safe criteria. Also, the radiation hazard parameters such as radium equivalent activity, absorbed gamma dose rate, outdoor and indoor annual effective dose equivalent, external and internal radiation hazard index, gamma index level, annual gonadal dose equivalent and excess lifetime cancer risk. All of these parameters are acceptable and within the worldwide values. The obtained results could be considered as reference data to follow up any changes in the future for natural radionuclides pollutants and their risks in the study area.

Cite this article: Hussien, M. T., Salaheldin, Gh., Salaheldin Mohamed, H., & Mansour, H. (2023). *Distribution of Natural Radionuclides and their Radiological Risks on Agricultural Soil Samples collected from Yemen.* Pollution, 2023, 9(1): 195-210.
http//doi.org/10.22059/poll.2022.344502.1507

DOI: http//doi.org/10.22059/poll.2022.344502.1507

INTRODUCTION

Uranium deposits contain naturally occurring uranium, which is extracted and converted into nuclear materials for both military and non-military use. while nuclear fuel consumption has increased activities for mining and processing uranium have been widely carried out over the last five years (Yuanyuan et al., 2021). The movement and leaching of natural deposits, releases from the mining sector, and use of phosphate fertilizers are all responsible for the existence and spread of uranium in the environment (Patra et al., 2013). The amount of naturally radioactive materials in the environment has lately increased due to a number of human activities, including nuclear weapon testing, the construction of nuclear power plants, and the fabrication and use of radioactive sources. Radiation-emitting substances may enter surface waters through a variety of processes or actions. By carrying radionuclides from metropolitan areas, mine waste, soil weathering, and agricultural areas, surface runoff from rain can damage waterways (Pujol &

*Corresponding Author Email: *ghadasalaheldin@aun.edu.eg*

Cabeza, 2000).

The use of radioactive materials in our daily lives, in general, has become widespread, so humans are exposed to doses that may affect their health, so physicists must identify these radionuclides, which constitute a significant cause of the spread of all kinds of cancers. Instead of looking behind the treatment, we must first start with the reasons and try to develop solutions to reduce its effects (Yang et al., 2005; Tsabaris et al., 2007; Alashrah et al., 2018). It is possible to divide the sources of radioactive materials into two parts, one of which is derived from nature and the other is artificial. The natural radioactive materials depend on soil geology components, which arose from the beginning of the earth's formation, and it is a specific and known quantity. It does not affect the environment or living organisms. Still, it prevents some diseases and epidemics that living organisms would perish if they spread on the earth, from a peaceful or military point of view (Dugalic et al., 2010). A substantial source of artificial source is Nuclear bomb tests and ^{137}Cs produced artificially as a result of the Chernobyl Accident (Miroslaw & Shinji, 2009).

Adagunodo et al., 2019 were assessed the radiological dangers associated with farmers' exposure to radionuclides, the distribution of radioactivity concentrations of thorium, uranium, and potassium were examined in soil samples randomly selected from ten farm locations in Odo Oba, southwest Nigeria. The mean concentrations of uranium, thorium and potassium are 29.40, 44.25 and 1072.04 Bq kg^{-1}respectively.

In 26 surface soil samples from two different sites of Libya, the natural radioactive nuclides ^{238}U, ^{232}Th, and ^{40}K were quantified. The soil samples were taken in northwest Libya from two distinct agricultural fields is determined by Alajeeli et al., 2019. The activity concentrations of uranium, thorium and potassium are 14.14, 14.31 and 359.8 Bq kg^{-1} respectively.

Ghazwa et al., 2016 measured the activity concentrations of the naturally occurring radionuclides ^{226}Ra, ^{232}Th, and ^{40}K in 30 agricultural and virgin soil samples randomly obtained from Kedah, Malaysia's northernmost state, at a fertile soil depth of 0–30 cm. ^{226}Ra, ^{232}Th, and ^{40}K were found to have mean radioactivity concentrations of 65.24, 83.39 and 136.98 Bq/ kg, respectively. Issa, 2013 measured the activity concentrations of the naturally occurring radionuclides 226Ra, 232Th, and 40K in Egypt and the obtained results of the activity concentration of 226Ra, ^{232}Th, and ^{40}K were 43, 54 and 183 respectively.

This absurdity creating environmental imbalances, we will reap everything wrong and not progress as some think. Since the primary source of radioelements in the environment is the soil, it supplies the plant with the nutrients needed for its growth (Wilcke, 2007; Alnagran, 2022). So we relied in our current research on measured and identification of radioactive elements in the soil from two regions of Yemen and calculated exposure risks by global equations. In agriculture, Yemen depends on rainwater and groundwater, which may increase radioactive contamination of the soil and crops (Wahib et al., 2022).

MATERIALS AND METHODS

The research area (Wadi Al-Hussini and Tuban) is in the southern region of Yemen, within the administrative center of Lahj. The governorate of Lahj is in Yemen's southwestern Republic, at latitudes of 12° 30' to 14° 00' N and longitudes of 43° 30' to 45° 30' E, some 775 kilometers from the capital. The Al-Bayda, Al-Dhalaa, and some parts of the Taiz borders are on the north, the Abyan on the east, the Taiz on the west, and the Gulf of Aden on the south, as shown in Figure 1. In general, Lahj is located on the Wadi Al-Hussini and Tuban Delta and is known for agriculture, the province's principal activity, accounting for 3.7 percent of total agricultural production in the Republic and producing the most significant feed and vegetables.

Many studies describe Yemen's geology, it comprises loess overlying Paleozoic, Mesozoic, and Cenozoic sediments, as well as exceedingly old metamorphic and crystalline igneous rocks. The

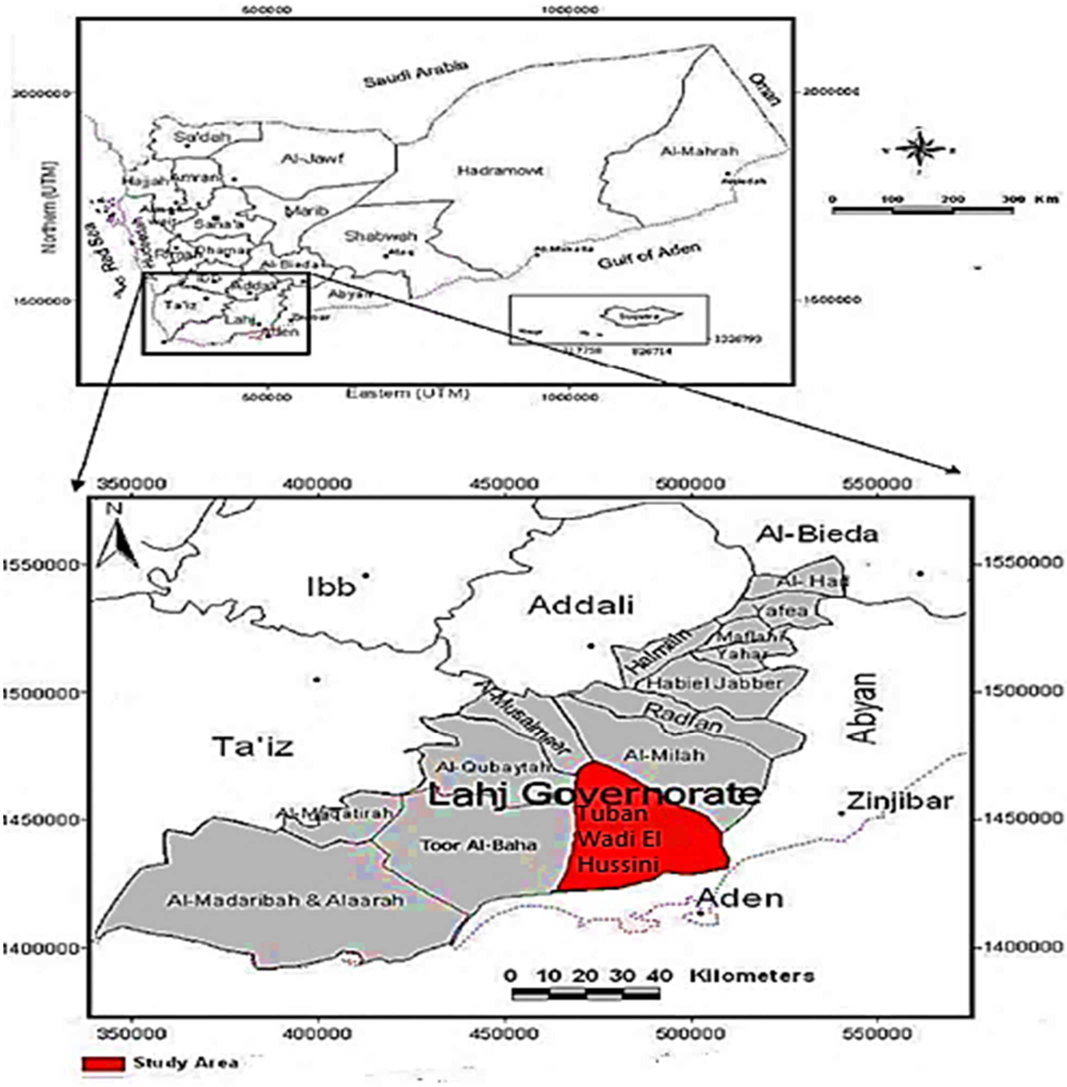

Fig. 1. Geologic map of the study area.

geological history of Yemen has been significantly influenced by erosion, which over time has destroyed a number of rock units. (Beydoun, 1966; Mattash, 1994; Menzies et al., 1994; Beydoun et al., 1998; As-Saruri, 1999; Wahib et al., 2022). The coastal plain, desert (southern section), and high land platform, mountains make up the terrain of Yemen's southern part (Western part) (northeast and, northwest and west). A range of flood plains produced along a big wadi, such as the Wadi Al-Hussaini and Tuban, is the Wadi plain when the Wadi cuts out of the mountains. The majority of the sediments in this study are Quaternary in age. The quaternary range is generally separated into basaltic lava and scoria dispersed along coastal and Wadi plain sand and gravel. The coastal plain and the Wadi plain deposits are mostly sand and gravel, with wind covering the area.

Forty samples were collected randomly from two regions of Yemen. Twenty samples from Tuban and the others from Wadi Al-Hussini. The samples weight nearly 500 gm, then sieved to become homogenized, then sealed in a specific beaker (marinelli) and stored about one month for a secular equilibrium between radium and its daughters. Researches using hyper pure germanium system to measure the activity concentration from photo peak energy, they use theoretical calculations to identify the risks parameters such as dose rate, radium equivalent, internal and external radiation hazard, Gamma index (I_γ), Annual gonadal dose equivalent and Excess lifetime cancer risk (ELCR).

Theoretical calculation

The calculated activity concentration in Becquerel per kilogram AC (Bq/kg) was measured as the following equation (Alashrah et al., 2018):

$$AC\left(Bq/kg\right)=\left[1/\varepsilon\left(C_{\grave{o}}-C_{B}\right)\right]/\left(\beta.M_{s}\right) \tag{1}$$

Where ε is the calculated efficiency for each photo peak energies, C_ϵ and C_B are counts per second for each photo peak energy for samples and background respectively, β is the probability of the disintegration and M_s is mass of sample in kilogram.

Equivalent activity of radium (Ra-eq) in Bq/kg was calculated by (Najam et al., 2017; El-Taher et al., 2019; Alnagran, 2022; Adagunodo et al., 2018) as:

$$\text{Ra-eq (Bq/kg)} = AC(Ra)+1.43AC(Th)+ 0.077AC(K) \tag{2}$$

Where AC is the activity concentration for ^{226}Ra, ^{232}Th and ^{40}K in sequence. Absorbed gamma dose rate (D-nGy/h) was determined and calculated by (Jibiri et al., 2007; UNSCEAR, 2008; Salaheldin et al., 2020; El-Azeem & Mansour, 2021; El-Taher & Al-Zahrani, 2014; Ibraheem et al., 2018) as the following:

$$D\ (nGy/h) = X_1C_1+X_2C_2+X_3C_3 \tag{3}$$

Where X_1, X_2 and X_3 equal 0.462, 0.604 and 0.0417 respectively. C_1, C_2 and C_3 are the activities for Ra-226, Th-232 and K-40 in sequences. Annual effective dose equivalent (AEDE) indoor and outdoor were calculated by (Oni et al., 2011; Huang et al., 2015; Ibitola et al., 2018; Ilori et al., 2020& 2021; Salaheldin et al., 2021) as the following equation:

$$AEDE\ (mSv/y) = D(nGy/h)*8760*0.7Sv/Gy*T_S*10^{-6} \tag{4}$$

Where T_S is the time stay over a year and equal 0.2, 0.8 for outdoors and indoors respectively.0.7 is the conversion factor. (D-nGy/h) is the absorbed dose in nGy/h.

Gamma level index (I_γ) can utilized to evaluate the level the hazard level of gamma radiation from γ-emitted by natural radionuclides (Ra-226, Th-232 and K-40). Gamma level index were calculated by Equation (5): (Adagunodo et al., 2021).

$$I_\gamma=\frac{AC(Ra)}{150}+\frac{AC(Th)}{100}+\frac{Ac(K)}{1500} \tag{5}$$

Where AC(Ra), AC(Th) and AC(K) are the activity concentration for Ra-226, Th-232 and K-40 in sequences.

Excess life time cancer risk presents the likelihood of creating cancer over a lifetime at a given exposure level, the number of more cancers anticipated in a given number of individuals on introduction to a carcinogen at a given dosage when the event that considering 70 years as the normal mean duration life for human being. It was calculated as the following equation:(Najam et al., 2015; El-Taher et al., 2021; Najam et al., 2022; Adagunodo et al., 2021).

$$ELCR = (AEDE\text{-}Sv/y) * DL(y) * RF(Sv) \tag{6}$$

Where DL(y) is duration of life and equal 70 years, RF(Sv) is risk cancer factor per Severt and equal 0.05 for the global report (ICRP, 1990).

Annual Gonadal Equivalent Dose (AGED) in order to determine how exposed human organs are to naturally occurring radionuclides, the gonad, bone marrow, and bone surface cells are crucial. Because farm activities take more time to complete, it is essential to incorporate AGED as part of our assessment of farmers' exposure to natural radionuclides. As a result, it's necessary to estimate the amount of AGED coming from the farmland. AGED were calculated according to Equation (7): (Adagunodo et al., 2019).

$$AGED\ (\mu Sv\ y\text{-}1) = 3{,}09\ AC(Ra) + 4{,}18\ AC(Th) + 0{,}314\ AC(K) \quad (7)$$

The data of activity concentration were analyzed using SPSS program in order to analyze the relationship between the variables used in this study, the descriptive analysis and multivariate statistics were used in this part. In recent years, the literature has found that this strategy is effective. Figures 6, 7 and 8 displays variations in the mean, standard deviation, skewness, kurtosis, and the overall average of all the variables. Data set distributions are classified as symmetric or asymmetric based on their skewness. Skewness is always zero for a normal distribution and almost equals zero for symmetric data. The data is skewed left when the skewness has a negative value, and vice versa. The kurtosis gauges a normal distribution's "tailedness," or whether it is heavy- or light-tailed (Adagunodo et al., 2019).

Table 1. Activity distribution of radionuclides (Bq/kg) and related hazard assessments for Wadi Al-Hussini.

Sample code no.	Activity (Bq/kg)			Ra-eq (Bq/kg)	H_{ex}	H_{in}	I_{γ}
	Ra-226	Th-232	K-40				
A1	52.09	33.64	1135.60	187.64	0.51	0.65	1.44
A2	73.29	34.70	882.39	190.86	0.52	0.71	1.42
A3	51.27	36.13	1021.59	181.60	0.49	0.63	1.38
A4	61.92	42.29	879.10	190.08	0.51	0.68	1.42
A5	55.23	21.20	1284.81	155.89	0.42	0.57	1.24
A6	74.44	32.76	1088.65	205.11	0.55	0.76	1.55
A7	46.41	24.41	962.91	155.46	0.42	0.55	1.20
A8	66.61	33.60	987.16	190.68	0.52	0.70	1.44
A9	67.11	39.02	1026.98	201.98	0.55	0.73	1.52
A10	60.27	26.66	959.38	172.27	0.47	0.63	1.31
A11	59.01	22.91	1013.33	169.81	0.46	0.62	1.30
A12	52.59	23.53	1064.36	168.18	0.45	0.60	1.30
A13	70.67	44.58	1005.02	211.80	0.57	0.76	1.59
A14	75.12	30.58	1045.66	199.37	0.54	0.74	1.50
A15	61.84	24.78	1150.79	185.89	0.50	0.67	1.43
A16	52.71	21.48	982.42	159.08	0.43	0.57	1.22
A17	64.35	29.72	1148.00	195.24	0.53	0.70	1.49
A18	62.60	31.14	1172.30	197.40	0.53	0.70	1.51
A19	61.63	34.41	1114.95	196.69	0.53	0.70	1.50
A20	69.91	33.78	977.89	193.51	0.52	0.71	1.46
Minimum	46.41	21.20	879.10	155.46	0.42	0.55	1.20
Maximum	75.12	44.58	1284.81	211.80	0.57	0.76	1.59
Average	61.95	32.89	1045.16	185.43	0.50	0.67	1.41
Stand. dev	8.38	6.37	101.09	15.60	0.042	0.06	0.11

RESULTS AND DISCUSSION

The current study is the determination and distribution of radionuclides in the two most important agricultural areas in Yemen (Wadi Al-Hussini and Tuban). Twenty samples were collected from Wadi Al-Hussini (Region A) and 20 from Tuban (Region T). Tables 1, 2 represent the activity distribution of radionuclides (Bq/kg) and related hazard assessments for Wadi Al-Hussini and Tuban. Through the results recorded in Tables 1, 2, it is clear that a high value in potassium-40 nuclides values compared with a global magnitude of 400 Bq/kg (ICRP, 1990; UNSCEAR, 2000), as the values fall in the range between 879.10 to 1284.81with arithmetic mean 1045.17±101.09 Bq/kg for region A and between 859.59 to 1186.89 with arithmetic mean 1078.13±76.44 Bq/kg for region T. The comparison of radioactivity concentration for ^{40}K in Bq/kg between region A and T was represented in Figure 2.

Also, a slight increase in radium-226 was noticed when compared with the global limit (17 to 60 Bq/kg) with average 39 Bq/kg (UNSCEAR, 2008), which ranges from 46.41to 75.12 with an arithmetic mean of 61.95±8.38 Bq/kg for Region A. It ranges from 47.84 to 85.48 with the arithmetic suggestion of 65.20±10.09 Bq/kg for Region T. These results are a little higher than the global limits and the reason for that is may be the geological formation. Figure 3 shows the radioactivity concentration in Bq/kg for ^{226}Ra between regions A and T.

It is clear that thorium-232 ranges between 21.20 to 44.58 with an arithmetic mean of 32.89

Table 2. Activity distribution of radionuclides (Bq/kg) and related hazard assessments for Tuban.

Sample code no.	Activity (Bq/kg)			Ra-eq (Bq/kg)	H_{ex}	H_{in}	I_{γ}
	Ra-226	Th-232	K-40				
T1	59.73	46.55	1034.42	205.95	0.56	0.72	1.55
T2	80.25	56.11	1081.18	243.74	0.66	0.88	1.82
T3	56.30	47.65	1133.74	211.73	0.57	0.72	1.61
T4	48.46	42.19	1079.19	191.89	0.52	0.65	1.46
T5	68.17	61.94	1166.91	246.60	0.67	0.85	1.85
T6	65.35	60.45	1053.69	232.92	0.63	0.81	1.74
T7	69.55	40.98	1037.83	208.07	0.56	0.75	1.57
T8	69.55	54.06	1166.01	236.64	0.64	0.83	1.78
T9	65.78	55.00	1042.73	224.71	0.61	0.78	1.68
T10	63.91	46.14	1060.96	211.59	0.57	0.74	1.59
T11	61.89	40.04	1046.63	199.74	0.54	0.71	1.51
T12	60.74	47.32	1160.56	217.77	0.59	0.75	1.65
T13	50.01	41.10	859.59	174.97	0.47	0.61	1.32
T14	64.98	54.64	1117.20	229.13	0.62	0.79	1.72
T15	47.84	24.75	1103.53	168.21	0.45	0.58	1.30
T16	79.78	65.92	1149.81	262.58	0.71	0.92	1.96
T17	65.48	51.00	1038.35	218.36	0.59	0.77	1.64
T18	85.48	64.30	1066.38	259.54	0.70	0.93	1.92
T19	74.45	75.35	976.97	257.42	0.70	0.90	1.90
T20	66.32	43.54	1186.89	219.98	0.59	0.77	1.67
Minimum	47.84	24.75	859.59	168.21	0.45	0.58	1.30
Maximum	85.48	75.35	1186.89	262.58	0.71	0.93	1.96
Average	65.20	50.95	1078.13	221.08	0.60	0.77	1.66
Stand. dev	10.09	11.41	76.44	26.13	0.07	0.10	0.18

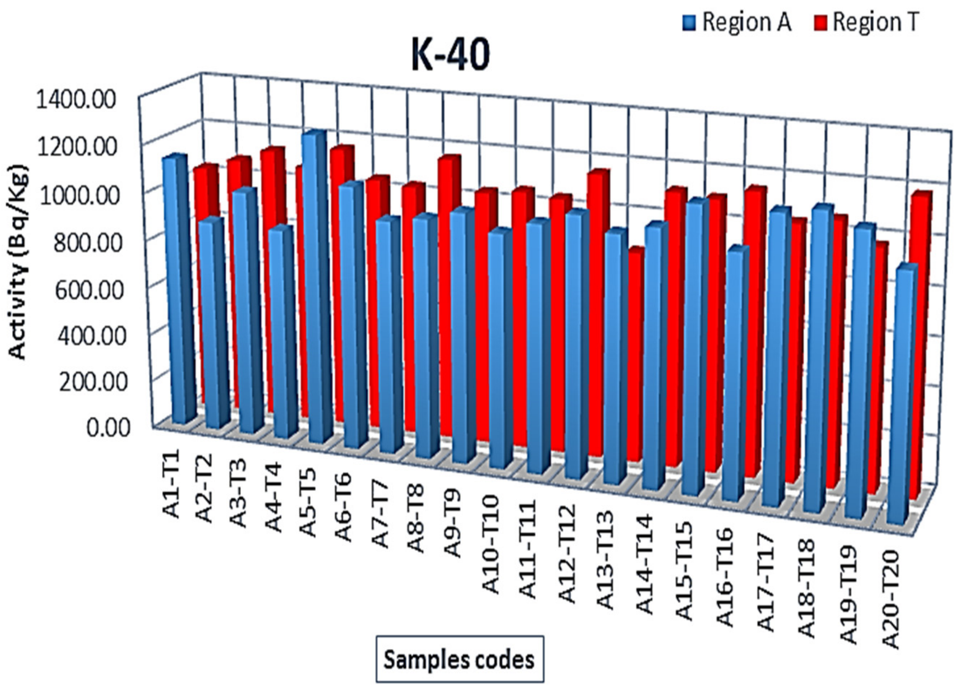

Fig. 2. Represents the variation of activity concentration of K-40 for region A and T.

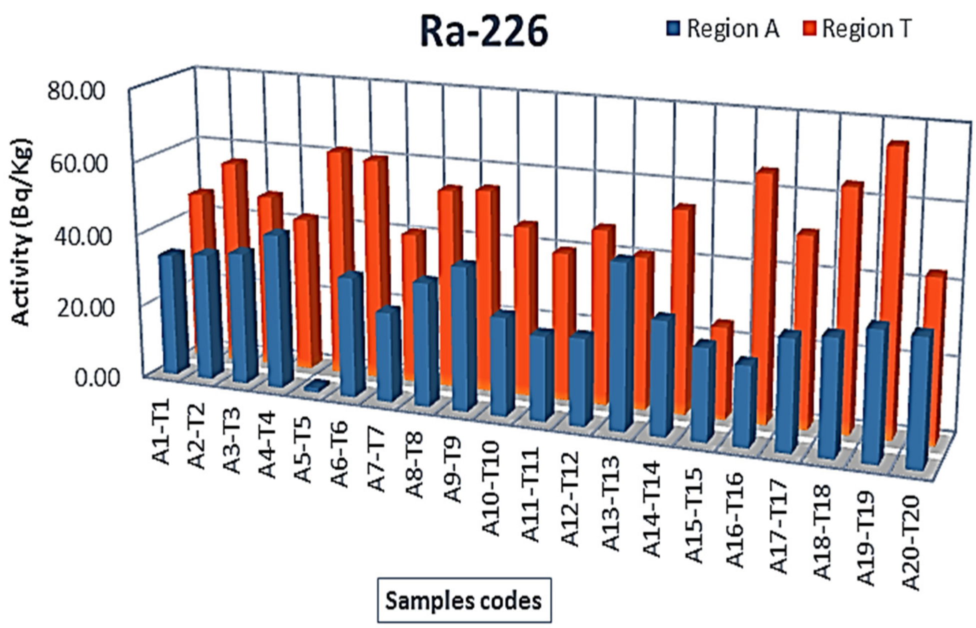

Fig. 3. Represents the variation of activity concentration of Ra-226 for region A and T

± 6.37 Bq/kg for Region A, and it ranges between 24.75 to 75.35 with an arithmetic mean of 50.95±11.41 Bq/kg for Region T. It seems that the results are within the limit compared to global values 11 to 68 Bq/kg (UNSCEAR, 2008) for Region A, the comparison of radioactivity concentration (Bq/kg) for ^{232}Th between region A and T is in Figure 4.

Radium equivalent activity (Bq/kg) was calculated and presented in Tables 1 and 2 for the

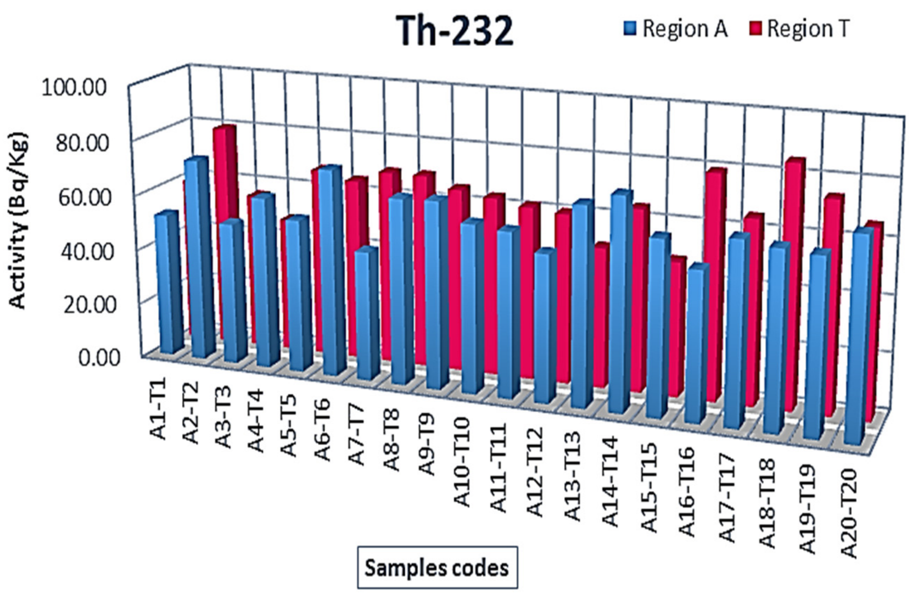

Fig. 4. Represents the variation of activity concentration of Th-232 for region A and T

Table 3. Calculated absorbed dose rate, effective dose (indoor-outdoor), annual dose and excess lifetime cancer risk for region A

Sample code no.	D (nGy/h)	$AEDE_{out}$ (mSv/y)	$AEDE_{in}$ (mSv/y)	AGDE (mSv/y)	ELCRx10^{-3}
A1	91.74	0.11	0.45	0.66	0.16
A2	91.62	0.11	0.45	0.65	0.16
A3	88.11	0.11	0.43	0.63	0.15
A4	90.81	0.11	0.45	0.64	0.16
A5	79.82	0.10	0.39	0.58	0.14
A6	99.58	0.12	0.49	0.71	0.17
A7	76.34	0.09	0.37	0.55	0.13
A8	92.24	0.11	0.45	0.66	0.16
A9	97.39	0.12	0.48	0.69	0.17
A10	83.95	0.10	0.41	0.60	0.14
A11	83.36	0.10	0.41	0.60	0.14
A12	82.89	0.10	0.41	0.60	0.14
A13	101.48	0.12	0.50	0.72	0.17
A14	96.78	0.12	0.47	0.69	0.17
A15	91.53	0.11	0.45	0.66	0.16
A16	78.30	0.10	0.38	0.56	0.13
A17	95.55	0.12	0.47	0.68	0.16
A18	96.61	0.12	0.47	0.69	0.17
A19	95.75	0.12	0.47	0.68	0.16
A20	93.48	0.11	0.46	0.66	0.16
Minimum	76.34	0.09	0.37	0.55	0.13
Maximum	101.48	0.12	0.50	0.72	0.17
Average	90.37	0.11	0.44	0.65	0.16
Stand. dev	7.19	8.82	35.28	50.39	0.12

two regions. It describes gamma radiation output from different radionuclides in soil samples. It fluctuated from 155.46 to 211.80 with an average of 185.43 Bq/kg for region A and from 168.21 to 262.58 with an average of 221.08 Bq/kg for region T. These results are lower than the permissible global magnitude of 370 Bq/kg (UNSCEAR, 2000).

The hazard parameters for each sample were determined through calculated external radiation hazard index (H_{ex}), internal hazard index (H_{in}), and gamma index level (I_{γ}), and these results were recorded in Tables 1, 2.

It is clear from the results that H_{ex} ranges from 0.42 to 0.57 with a mean of 0.50, H_{in} ranges from 0.55 to 0.76 with a mean of 0.67, and I_{γ} ranges from 1.20 to 1.59 with a mean of 1.41 for region A. The region T found that H_{ex} ranges from 1.30 to 1.96 with a mean of 1.66, H_{in} ranges from 0.58 to 0.93 with a mean of 0.77, and I_{γ} ranges from 0.65 to 0.98 with a mean of 0.83.

Tables 3 and 4 represent calculated absorbed dose rate, annual effective dose (indoor – outdoor) and excess lifetime cancer risk. In the current study, the absorbed dose rate of region A is from 76.34 to 101.37 with a mean of 90.37 nGy/h, but region T ranges from 83.07 to 124.62 with a mean of 105.86 nGy/h. The results of the two regions are higher than the global ranges; this rise in magnitude is due to the increased activity concentration of some radionuclides as ^{40}K. Region T is nearly higher than region A because of the increase in radionuclide concentration. Due to the nature of the geological region.

The annual effective dose equivalent outdoor and indoor for each sample were calculated using equation written by (El-Taher & Al-Zahrani, 2014) and presented in Tables 3 and 4. The

Table 4. Calculated absorbed dose rate, effective dose (indoor-outdoor), annual dose and excess lifetime cancer risk for region T

Sample code no.	D (nGy/h)	$AEDE_{out}$ (mSv/y)	$AEDE_{in}$ (mSv/y)	AGDE (mSv/y)	ELCRx10^{-3}
T1	98.85	0.12	0.48	0.70	0.17
T2	116.05	0.14	0.57	0.82	0.20
T3	102.07	0.13	0.50	0.73	0.18
T4	92.88	0.11	0.46	0.66	0.16
T5	117.57	0.14	0.58	0.84	0.20
T6	110.64	0.14	0.54	0.79	0.19
T7	100.16	0.12	0.49	0.71	0.17
T8	113.41	0.14	0.56	0.81	0.19
T9	107.09	0.13	0.53	0.76	0.18
T10	101.64	0.12	0.50	0.72	0.17
T11	96.42	0.12	0.47	0.69	0.17
T12	105.04	0.13	0.52	0.75	0.18
T13	83.77	0.10	0.41	0.60	0.14
T14	109.61	0.13	0.54	0.78	0.19
T15	83.07	0.10	0.41	0.60	0.14
T16	124.62	0.15	0.61	0.88	0.21
T17	104.36	0.13	0.51	0.74	0.18
T18	122.80	0.15	0.60	0.87	0.21
T19	120.64	0.15	0.59	0.85	0.21
T20	106.43	0.13	0.52	0.76	0.18
Minimum	83.07	0.10	0.41	0.60	0.14
Maximum	124.62	0.15	0.61	0.88	0.21
Average	105.86	0.13	0.52	0.75	0.18
Stand. dev	11.64	14.28	57.11	80.35	0. 20

annual effective dose equivalent on a worldwide value is 0.41 mSv/y, of which 0.07 mSv/y comes from outdoor exposure and 0.34 mSv/y from outdoor. Thus, most results are nearly normal with the global average where (AEDE out) ranges from 0.09 to 0.12 with mean 0.11 and (AEDE in) ranges from 0.37 to 0.50 with mean 0.44 for region A but (AEDE out) ranges from 0.10 to 0.15 with mean 0.13 and (AEDE in) ranges from 0.41 to 0.61with mean 0.52 for region T.

The annual gonadal dose equivalent (AGDE) was calculated and presented in Tables 3 and 4. For region A, the values lie between 0.55 and 0.75 with a mean of 0.65, but for region T, it lies between 0.60 to 0.88 with a mean of 0.75.

The increase of excess lifetime cancer risk (ELCR) raises the chance of developing cancer due to direct exposure to harmful substances brought almost over an individual's lifetime. The ELCR was calculated and ranged from 0.13×10^{-3} to 0.17×10^{-3} with an average 0.16×10^{-3} for region A while it ranged from 0.14×10^{-3} to 0.21×10^{-3} with average 0.18×10^{-3} for region T. The current study showed that the mean values for both regions A and T are lower than the global mean which equal 0.29×10^{-3} (UNSCEAR, 2000). These indicate safety exposure in both regions.

With the Alpha GUARD Radon Detector, the average activity concentrations in regions A and T of ^{222}Rn were measured to be 5170±1740 and 7263±2061 Bq m^{-3}, respectively ((Salaheldin et al., 2020). As shown in Figure 5, there are strong and moderate associations between most ^{222}Rn against ^{226}Ra values, with R= 0.5059 and R= 0.3041 in regions A and T, respectively. Due to their occurrence in the same decay sequence as uranium (^{238}U), where radon is the product of radium, the relationship between radium (^{226}Ra) and radon (^{222}Rn) exhibited a high positive correlation.

As shown in table 6, when the findings of activity concentration of radionuclides in this study were compared to those from other studies conducted in Yemen and other regions of the world, with the exception of a few situations, their conclusions were found to be in agreement.

Descriptive statistics of natural radionuclides

The Gaussian frequency distribution curve for radium equivalent activity in Bq/kg is plotted for regions A and T as shown in Figure 6. that is clear that a nearly close Gaussian distribution curve for regions A, T. From the descriptive statistics of the frequency curve, the skewness equals -0.558 and -0.308; kurtosis equals -0.687 and -0.255 for regions A and T in sequence. The mean and median equal 185.43 and 190.38, with a standard deviation equal to 16.64 for region A and 105.86. The mean and median equal 105.86 and 105.74, with a standard deviation equal to 11.64

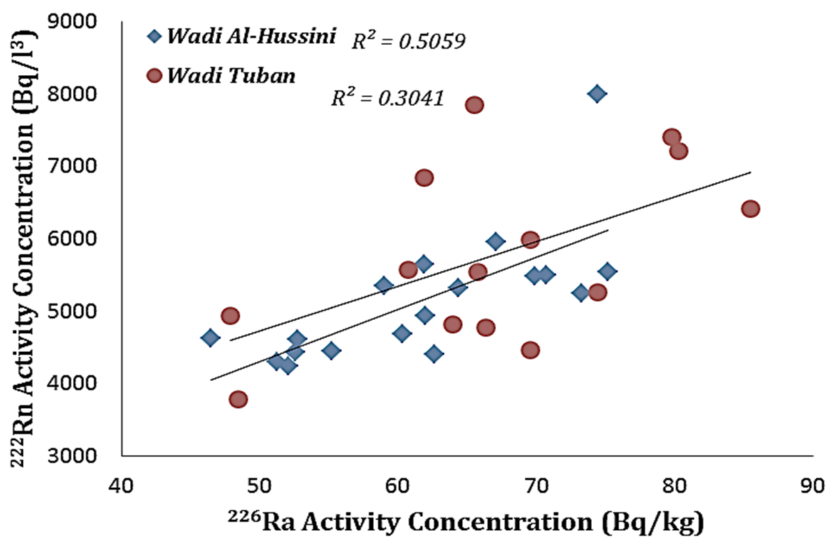

Fig. 5. Correlations between ^{226}Ra and ^{222}Rn of the samples under investigation

Table 5. Mean values and variance with ANOVA table for the radon concentration components in the groups (A-D) of Wadi Al-Hussini and Tuban.

radionuclides	Groups	A	B	C	D	P-value
	Count	**5**	**12**	**7**	**16**	
Ra-226	Sum	312.72	738.55	478.67	1013.16	0.488528
	Average	62.55	61.546	68.38	63.32	
	Variance	104.62	74.49	44.22	110.51	
Th-232	Sum	287.58	566.56	214.99	585.08	0.000209
	Average	57.52	47.21	30.71	36.57	
	Variance	169.57	92.78	19.19	149.27	
K-40	Sum	5410.50	13071.62	6954.46	17029.26	0.141282
	Average	1082.1	1089.30	993.49	1064.33	
	Variance	5431.99	11063.78	4326.78	6851.50	

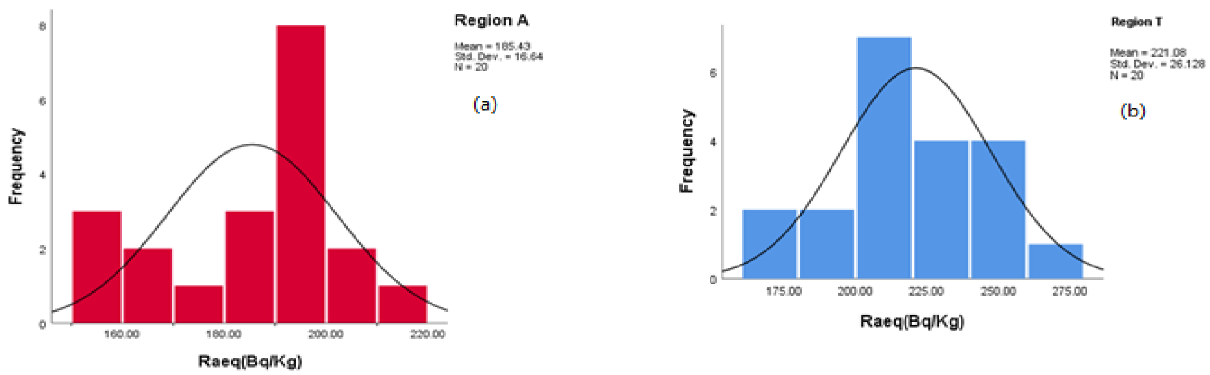

Fig. 6. The Gaussian frequency distribution curve for radium equivalent activity (Bq/kg) for (a) region A and (b) region T

for region T. the variance equal 246.88 and 135.57 for region A and T in sequence.

Figure 7. represents the Gaussian frequency curve of absorbed dose rate (nGy/h). It is clear that a nearly close to symmetric distribution with skewness equal -0.505, kurtosis equal -0.781 for region A and skewness equal -0.308, kurtosis equal -0.255 for region T. In contrast, region T is more symmetric than region A.

Cluster Analysis

Cluster analysis of radionuclide concentrations on levels of radioactivity in agricultural soil was performed using the PAST computer software. The goal of cluster analysis is to classify system items based on cluster similarity and to discover the best grouping of things that are similar to each other but not identical.

The classification of radioactive activity concentrations (^{226}Ra, ^{232}Th, and ^{40}K) recorded in 40 stands Wadi Al-Hussini (Region A) and Tuban (Region T) in the current study. By using cluster analysis as shown in Table 5, four groups were generated at the second level of the hierarchy in Figure 8. Group (A) comprised five stands, with an average value and variance of (62.5448 and 104.6244), (57.515 and 169.5669), and (1082.1 and 5431.995) for ^{226}Ra, ^{232}Th, and ^{40}K, respectively. Group (B) comprised twelve stands, with an average value and variance of (61.56 and 74.49), (47.21 and 92.78), and (1089.30, and 11063.78) for ^{226}Ra, ^{232}Th, and ^{40}K, respectively. Group (C) comprised seven stands, with an average value and variance of (68.38 and 44.22),

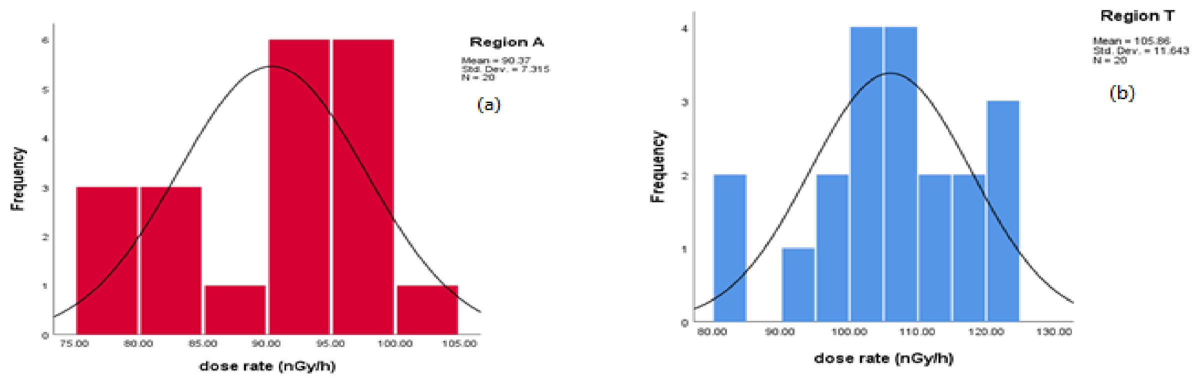

Fig. 7 The Gaussian frequency curve of absorbed dose rate (nGy/h) for (a) region A and (b) region T

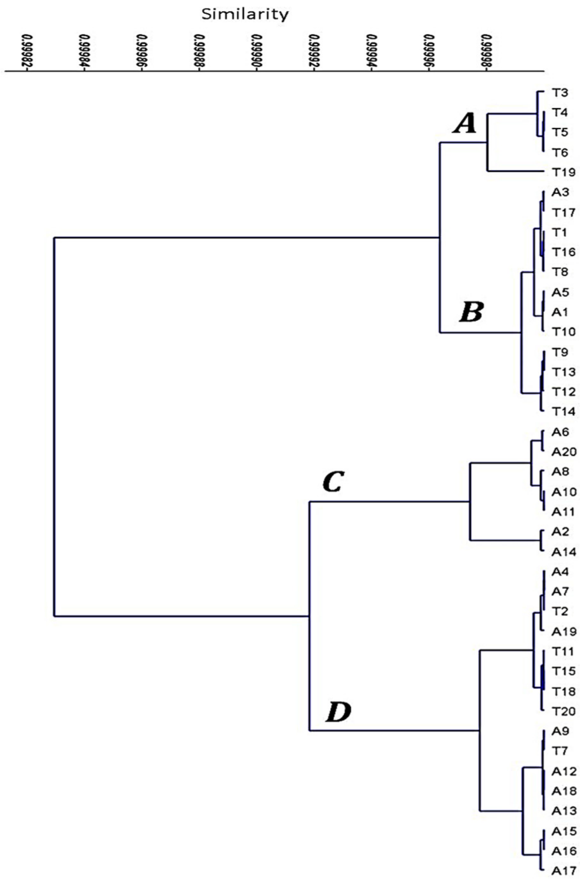

Fig. 8. Cluster analysis of region A and T

(30.71 and 19.19), and (993.49, and 4326.78) for ^{226}Ra, ^{232}Th, and ^{40}K, respectively. Group (D) comprised sixteen stands, with an average value and variance of (63.32 and 110.51), (36.58 and 149.27), and (1064.33 and 6851.50) for ^{226}Ra, ^{232}Th, and ^{40}K, respectively.

As shown in Table 5, there is no significant difference among the four groups in case of the radioactive of ^{226}Ra and ^{40}K. This indicates that there is no difference of groups that may be the result of the same soil components in two regions Wadi Al-Hussini and Tuban. On the other side, p-value is significantly different among the four groups in case of the radioactive of 232Th.

Distribution of radon concentration in study area

Based on a ^{226}Ra, ^{232}Th and ^{40}K distribution map of those agricultural soil samples collected

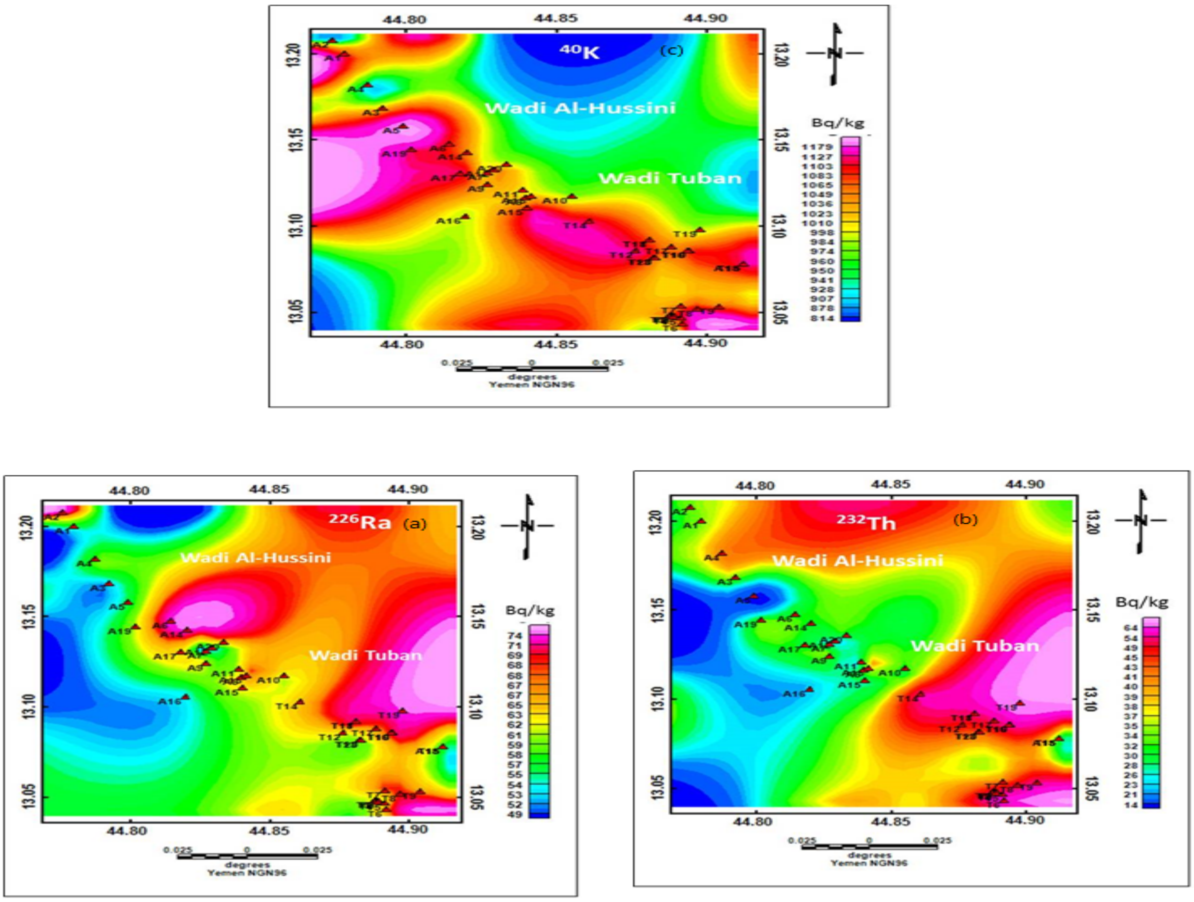

Fig. 9. Distribution map of concentrations for Wadi Al-Hussini and Wadi Tuban areas of (a) ^{226}Ra, (b) ^{232}Th and (c) ^{40}K

Table 6. Comparison of the present study of radioactivity concentration with other location.

Country	^{238}U or ^{226}Ra Bq/kg	^{232}Th Bq/kg	^{40}K Bq/kg	reference
Yemen				
Region A	61.95	32.89	1045.16	Present study
Region T	65.20	50.95	1078.13	
SW, Nigeria	29.40	44.25	1072.07	Adagunodo et al. 2019
India	19.16	48.56	1146.88	Chandrasekaran et al. 2014
Libya	14.14	14.31	359.8	Alajeeli et al. 2019
Malaysia	65.24	83.39	136.98	Ghazwa et al. 2016
Pakistan	30	56	602	Tufail et al. 2006
Algeria	53.2	50.03	311	Boukhenfouf and Boucenna, 2011
Egypt	43	54	183	Issa, 2013

from Wadi Al-Hussini and Wadi Tuban as in Figure 9 It has been found that there is a noticeable difference in ^{226}Ra, ^{232}Th and ^{40}K activity concentrations where the concentration natural radioactivity differs from one region to another. ^{226}Ra and ^{232}Th concentrations in Tuban district is higher than in Wadi Al-Hussini district, and on the other side ^{40}K concentration in Wadi Al-Hussini district is higher than in Wadi Tuban district.

CONCLUSION

The main goal of the current study is to measure and determine natural radionuclides (Ra-226, Th-232, and K-40) from terrestrial sources and detect the health risk of exposure of agricultural soil samples collected from two regions (Wadi Al-Hussini and Tuban) in Yemen. Forty samples were measured using a gamma spectroscopy system (HPGe-detector). The findings of the specific radioactivity concentration are in near agreement with worldwide publish for Ra-226 and Th-232 but higher than global ranges for K-40 in both study areas. When exposed over a prolonged period of time, it increases the health risks for the locals. In comparison to the worldwide ranges, the danger parameter recorded the typical magnitudes. Finally, the experts advise routinely monitoring the rising radionuclides and addressing the root causes of radioactive pollution. Natural radionuclide descriptive statistics agree with each other, with region T being more symmetric than region A. In the instance of the radioactive of ^{226}Ra and ^{40}K, cluster analysis revealed that the P-value is non significantly different among the observed four groups. This implies no difference in groups in the two regions, Wadi Al-Hussini and Tuban, which could be due to the identical soil components. In the case of radioactive ^{232}Th, however, P-value indicates significant differences among the observed four groups. According to the distribution map, the concentration of natural radioactivity varies from one place to the next in the current study. The findings could be used as a baseline for monitoring.

GRANT SUPPORT DETAILS

The present research did not receive any financial support.

CONFLICT OF INTEREST

The authors declare that there is not any conflict of interests regarding the publication of this manuscript.

LIFE SCIENCE REPORTING

No life science threat was practiced in this research.

REFERENCES

Alajeeli, A., Elmahroug, Y., Mohammed, S. and Trabelsi, A. (2019). Determination of natural radioactivity and radiological hazards in soil samples: Alhadba and Abuscabh agriculture projects in Libya. Environ. Earth Sci., 78; 1-8.

Alashrah, S., El-Taher, A. and Mansour, H. (2018). Assessment of radiological parameters and metal contents in soil and stone samples from Harrat Al Madinah, Saudi Arabia. MethodsX, 5; 485-494

Alnagran, H., Alashrah, S., Suardi, N. and Mansour, H. (2022). Study of Radionuclides and Assessment of Radioactive risks for Environmental particulate matters in Qassim region, Saudi Arabia. Pollution, 8(3); 1049-1060.

Adagunodo, T. A., Sunmonu, L. A., Adabanija, M. A., Omeje, M., Odetunmibi, O. A. and Ijeh, V. (2019). Statistical assessment of radiation exposure risks of farmers in Odo Oba, Southwestern Nigeria. Bull. Min. Res. Exp., 159; 201-217.

Adagunodo, T. A., Akinloye, M. K., Sunmonu, L. A., Aizebeokhai, A. P., Oyeyemi, K. D. and Abodunrin, F. O. (2018). Groundwater Exploration in Aaba Residential Area of Akure, Nigeria. Frontiers in Earth Science 6; 66.

Adagunodo, T. A., Enemuwe, C. A., Usikalu, M. R., Orosun, M. M., Adewoyin, O. O., Akinwumi, S. A., Oloke, O. C., Lukman, A. F., Adeniji, A. A. and Adewoye, A. O. (2021). Radiometric survey of natural radioactivity concentration and risk assessment on dwellers around Ijako active dumpsite in

Ogun State. IOP Conf. Series: Ear. and Enviro. Sci., 655; 1-7.
As-Saruri, M. (1999). Lithostratigraphie der Tertiär-Sedimente der Republik Jemen: Verlag der Gesellschaft für Geologische Wissenschaften.
Beydoun, Z. (1966). Geology of the Arabian Peninsula, eastern Aden Protectorate and part of Dhofar. United States Geological Survey Professional Paper, 560-H 49
Beydoun, Z., As-Saruri, A. L., Mustafa, E. H., Al-Ganad, I. N., Baraba, R. S., Nani, A. S. O. and Al-Aawah, M. H. (1998). International lexicon of stratigraphy, Volume III, Republic of Yemen, 2nd edn. In: International union of geological sciences and ministry of oil and mineral resources. Republic of Yemen Publication, 34; 245.
Chandrasankaran, A., Ravisankar, R., Senthilkumar, G., Thillaivelavan, K., Dhinakaran, B., Vijayagopal, P., Bramha, S. N. and Venkatraman, B. (2014). Spatial Distribution and Lifetime Cancer Risk due to Gamma Radioactivity in Yelagiri Hills, Tamilnadu, India. Egyptian Journal of Basic and Applied Science, 1; 38-48.
Dugalic, G., Krstic, D., Jelic, M., Nikezic, D., Milenkovic, B., Pucarevic, M. and Zeremski-Skoric, T. (2010). Heavy metals, organics and radioactivity in soil of western Serbia. Journal of hazardous materials, 177; 697-702
El-Azeem, A. and Mansour, H. (2021). Determination of natural radionuclides and mineral contents in environmental soil samples. Arabian Journal for Science and Engineering, 46; 697-704.
El-Taher, A. and Al-Zahrani, J. (2014). Radioactivity measurements and radiation dose assessments in soil of Al-Qassim region, Saudi Arabia. Ind. J. Pure Appl. Phys., 52; 147-154.
El-Taher, A., Badawy, W., Khater, A. and Madkour, H. (2019). Distribution patterns of natural radionuclides and rare earth elements in marine sediments from the Red Sea, Egypt. Applied Radiation and Isotopes, 151; 171-181.
El-Taher, A., Kamel, M., Tolba, A. and Salaheldin, G. (2021). Evaluation of natural radioactivity and radiological hazards in basement rocks from Gabel Abu El-Hassan in the North Eastern Desert of Egypt by multivariate statistical approach with remote sensing data. Radiation Detection Technology and Methods, 5; 15-26.
Ghazwa, A., Fauziah, B. S. H. and Abdul Rahman, I. (2016). Assessment of Natural Radioactivity Levels and Radiation Hazards in Agricultural and Virgin Soil in the State of Kedah, North of Malaysia. Hindawi Publishing Corporation, the Scientific World Journal, 1-9.
Huang, Y., Lu, X., Ding, X. and Feng, T. (2015). Natural radioactivity level in beach sand along the coast of Xiamen Island, China. Marine Pollution Bulletin, 91; 357-361.
Ibitola, A., Gilbert, A., Ilori, A., Aremu, R., Omosebi, I. (2018). Measurement of (^{40}K, ^{238}U and ^{232}Th) and associated dose rates in soil and commonly consumed foods (vegetables and tubers) at Okitipupa, Ondo State, Southwestern Nigeria. Asian Journal of Research and Reviews in Physics, 1; 1-11.
Ibraheem, A., El-Taher, A. and Alruwaili, M. (2018). Assessment of natural radioactivity levels and radiation hazard indices for soil samples from Abha, Saudi Arabia. Results in Physics, 11; 325-330.
ICRP (1990) Recommendations of the International Commission on Radiological Protection). ICRP Publication 60
Ilori, A., Chetty, N. and Adeleye, B. (2020). Activity concentration of natural radionuclides in sediments of Bree, Klein-Brak, Bakens, and uMngeni rivers and their associated radiation hazard indices. Transactions of the Royal Society of South Africa, 75; 258-265.
Ilori, A. and Chetty, N. (2021). Activity concentrations and radiological hazard assessments of ^{226}Ra, ^{232}Th, and ^{40}K in soil samples of oil-producing areas of South Africa. International Journal of Environmental Health Research, 1-13.
Issa S. (2013). Radiometric assessment of natural radioactivity levels of agricultural soil samples collected in Dakahlia, Egypt. Radiation Protection Dosimetry, 156(1); 59-67.
Jibiri, N., Farai, I. and Alausa, S. (2007). Estimation of annual effective dose due to natural radioactive elements in ingestion of foodstuffs in tin mining area of Jos-Plateau, Nigeria. Journal of Environmental Radioactivity, 94; 31-40.
Mattash, M. (1994). Study of the Cenozoic Volcanics and their associated intrusive rocks in Yemen in relation to rift development Hungarian Acad. Sci. Eötvös Loránd Univ. Budapest, 112.
Menzies, M., Al Kadasi, M., Al Khirbash, S., Al Subbary, A., Baker, J., Blakey, S., Bosence, D., Davison, I., Dart, C., Owen, L., Mcclay, K., Nicholls, G., Yelland, A. and Watchorn, F. (1994). Geology of the Republic of Yemen. Geology and Mineral Resources of Yemen: Geological Survey and Mineral Exploration Board, Yemen Mineral Sector Project Technical Report, 21-48.

Najam, L., Majeed, F., Kheder, M. and Younis, S. (2017). Estimation the Radiological Hazard Effects for Soil Samples of Nineveh Province. International Journal of Physics, 5; 53-56.

Najam, L., Younis, S. and Kithah, F. (2015). Natural radioactivity in soil samples in Nineveh Province and the associated radiation hazards. International Journal of Physics, 3; 126-132.

Najam, L. A., Mahmmod, R. H. and Albanna, O. M. J. (2022). Evaluation of Natural Radionuclides in Samples of Plant Fertilizers Used in Iraq and Radiation Hazard Indicators. Iran J. Sci. Technol. Trans Sci.

Miroslaw, J. and Shinji, T. (2009). Natural and Artificial Sources of Radioactivity in Poland. Jpn. J. Health Phys., 44 (1); 116-121.

Oni, O., Farai, I. and Awodugba, A. (2011). Natural radionuclide concentrations and radiological impact assessment of river sediments of the coastal areas of Nigeria. Journal of Environmental Protection, 2; 418-423.

Patra, A. C., Sahoo, S. K., Tripathi, R. M. and Puranik, V. D. (2013). Distribution of radionuclides in surface soils, Singhbhum Shear Zone, India and associated dose. Environ. Monit. Assess., 185; 7833-7843.

Pujol, L. I. and Sanchez-Cabeza, J. A. (2000). Natural and artificial radioactivity in surface waters of the Ebro river basin (Northeast Spain). Journal of Environmental Radioactivity, 51(2); 181-210.

Salaheldin, G., Elhaddad, M. and El-Gamal, H. (2021). Estimation of the natural radioactivity levels and rare earth elements concentration in the granitic rocks, Gabal Ghareb, Eastern Desert, Egypt. Environmental Earth Sciences, 80; 1-14.

Salaheldin, G., Hussien, M. and Mohamed, H. (2020). Evaluation of radiological hazards of radon in agricultural soil samples, Wadi Al-Hussini and Tuban, Lahj Governorate, Yemen. International Journal of Low Radiation, 11; 244-258.

Salaheldin, G., Tolba, A., Kamel, M. and El-Taher, A. (2020). Radiological hazard parameters of natural radionuclides for neoproterozoic rocks from Wadi Um Huytat in central eastern desert of Egypt. Journal of Radioanalytical and Nuclear Chemistry, 325; 397-408.

Tsabaris, C., Eleftheriou, G., Kapsimalis, V., Anagnostou, C., Vlastou, R., Durmishi, C., Kadhi, M. and Kalfas, C. (2007). Radioactivity levels of recent sediments in the Butrint Lagoon and the adjacent coast of Albania. Applied Radiation and Isotopes, 65; 445-453.

Tufail, M., Akhtar, N. and Waqas, M. (2006). Measurement of terrestrial radiation for assessment of gamma dose from cultivated and barren saline soils of Faisalabad in Pakistan, Radiation Measurements, 41(4); 443-451.

UNSCEAR (2000). United Nations Scientific Committee on the Effects of Atomic Radiation, Report to the General Assembly. United Nations, New York 2000.

UNSCEAR (2008). United Nations Scientific Committee on the Effect of Atomic Radiation. Sources and effects of ionizing radiation, New York.

Wahib, A., Fares, A., Henk, R., Ghunaim, N. and Petra, H. (2022). Natural and human-induced drivers of groundwater depletion in Wadi Zabid, Tihama coastal plain, Yemen. Journal of Environmental Planning and Management, 2; 1-22.

Wilcke, W. (2007). Global patterns of polycyclic aromatic hydrocarbons (PAHs) in soil. Geoderma, 141; 157-166.

Yang, Y., Wu, X., Jiang, Z., Wang, W., Lu, J., Lin, J., Wang, L. and Hsia, Y. (2005). Radioactivity concentrations in soils of the Xiazhuang granite area, China. Applied Radiation and Isotopes, 63; 255-259.

Yuanyuan, L., Weibo, Z., Bai, G., Zhihong, Z., Gongxin, C., Qianglin, W. and Ying, H. (2021). Determination of radionuclide concentration and radiological hazard in soil and water near the uranium tailings reservoir in China, Environmental Pollutants and Bioavailability, 33(1); 174-183.